2007 IEEE International Conference on
Robotics and Automation
Roma, Italy, 10-14 April 2007

A four-channel adaptive structure for high friction teleoperation systems in contact with soft environments.

Thomas Delwiche and Michel Kinnaert

***Abstract*— In this paper, an adaptive control structure based on the well-known four-channel (4C) control architecture is proposed to achieve transparency in non-ideal (high friction) teleoperation devices. The choice of the parameters to be adapted is motivated using a modified version of the 4C model. Next, two experiments are proposed to define the boundaries of the parameters values to be tuned during the adaptive process. Finally, the adaptive control scheme is successfully applied experimentally to a one degree of freedom (dof) teleoperation device.**

I. INTRODUCTION

Teleoperation consists in performing a remote task with an electromechanical master-slave device. The master part of the system is manipulated by the human operator while the slave part, which is located remotely, tries to perform the task imposed by the master. It is generally used in hazardous or narrow environments. The main applications of teleoperation include nuclear waste handling, undersea exploration and minimally invasive surgery (see [3]).

When force feedback is present at the master side to make the user feel the interaction forces between the slave and its environment, one refers to bilateral teleoperation. In bilateral teleoperation, the objective is to achieve the so-called transparency, i.e. to give the user the same feeling as if he or she was directly acting on the remote environment. In [10], transparency was defined in mathematical terms as having perfect position and force tracking for the largest possible bandwidth. To achieve this goal, the four-channel (4C) architecture, which is theoretically transparent, was introduced in [7]. In this control scheme, both positions and forces are measured and exchanged between the master and the slave. Another version of this control structure including local force loops around the master and the slave was studied by [6] and the benefits of local loops on stability were highlighted. This 4C scheme with local force loops is depicted in figure 1 in the case of a one degree of freedom (dof) device. The associated notations are: F_e, the net force exerted on the environment by the slave, F_h, the net force exerted by the user on the master, F_e^*, the active force exerted by the environment on the slave as opposed to a reaction force, F_h^*, the muscular force of the user, X_s, the position of the slave, X_m, the position of the master, F_m, the sum of F_h and the force provided by the actuator of the master ($F_{m,actuator}$) and F_s, the sum of $-F_e$ and the force provided by the actuator of the slave ($F_{s,actuator}$). Forces and positions can be related using the corresponding impedances which are ratios between the Laplace transform of the force applied on a mechanical system over the Laplace transform of its position: $F_e + F_e^* = Z_e X_s$, $F_h^* - F_h = Z_h X_m$, $F_s = Z_s X_s$, $F_m = Z_m X_m$.

Thomas Delwiche and Michel Kinnaert are with the Faculty of Applied Science, Department of Control Engineering and Systems Analysis, Université Libre de Bruxelles, CP165/55, Av. F.D. Roosevelt, B-1050 Brussels, Belgium. Emails: {Thomas.Delwiche,michel.kinnaert}@ulb.ac.be

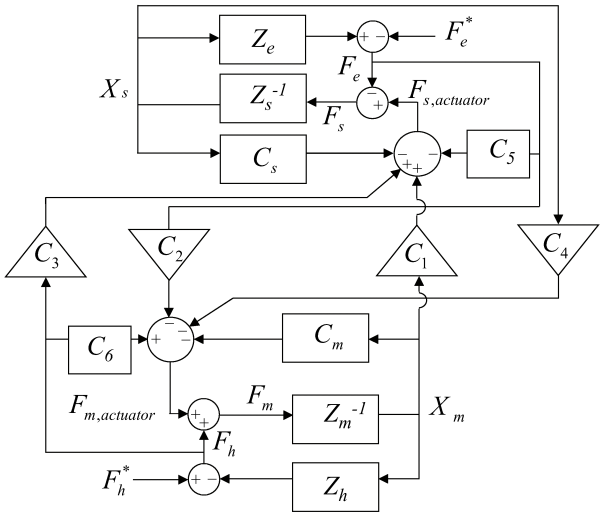

Fig. 1. Four channel control architecture including local force loops (C_5 and C_6)

If it is assumed that the system is linear (i.e. it can be modeled using Laplace transforms) and perfectly known, perfect transparency can be achieved when the four communication channels, denoted by C_1 to C_4 in figure 1, are chosen according to (1) (see [6]).

$$\begin{array}{ll} C_1 = C_s + Z_s & C_2 = C_6 + 1 \\ C_4 = -(C_m + Z_m) & C_3 = C_5 + 1 \end{array} \tag{1}$$

This can be proved using the hybrid representation of the teleoperation system, which was first introduced in [4] and which is defined by the following expression:

$$\begin{pmatrix} F_h \\ X_s \end{pmatrix} = \begin{pmatrix} h_{11} & h_{12} \\ h_{21} & h_{22} \end{pmatrix} \begin{pmatrix} X_m \\ F_e \end{pmatrix} \tag{2}$$

In the case of the 4C scheme of figure 1, the hybrid parameters are given by expressions (3) to (6).

$$h_{11} = \frac{(Z_m + C_m)(Z_s + C_s) + C_1 C_4}{(C_6 + 1)(Z_s + C_s) - C_3 C_4} \tag{3}$$

$$h_{12} = \frac{C_2(Z_s + C_s) - C_4(C_5 + 1)}{(C_6 + 1)(Z_s + C_s) - C_3 C_4} \tag{4}$$

$$h_{21} = \frac{C_3(Z_m + C_m) + (C_6 + 1)C_1}{(C_6 + 1)(Z_s + C_s) - C_3C_4} \quad (5)$$

$$h_{22} = \frac{C_2C_3 - (C_6 + 1)(C_5 + 1)}{(C_6 + 1)(Z_s + C_s) - C_3C_4} \quad (6)$$

If the expressions of (1) are substituted for C_1 to C_4 into the expressions of the hybrid parameters, then the hybrid matrix takes the form given by expression (7) below, which is the ideal one. Indeed the relations $F_h = F_e$ and $X_s = X_m$ are then obtained which corresponds to perfect transparency, according to [10].

$$H_{ideal} = \begin{pmatrix} 0 & 1 \\ 1 & 0 \end{pmatrix} \quad (7)$$

Unfortunately, perfect transparency can not be achieved. Indeed, the models $\hat{Z}_m$ and $\hat{Z}_s$ that can be substituted for Z_m and Z_s in (1) are subject to uncertainties preventing perfect dynamics compensation. Moreover, these expressions contain second order terms corresponding to the accelerations which are difficult to estimate based on the generally available position measurements.
Nevertheless, this scheme has been successfully implemented in [11] and [1]. By neglecting the higher order terms in (1), good low frequency performance were achieved as only the low order dynamics were compensated.

In this paper, the application of the 4C control scheme with local force loops in the case of non-ideal systems, i.e. high friction teleoperation devices, is addressed. It is shown experimentally that, if one sticks to a linear model, such a system is time-varying, which requires an adaptive control structure to keep suitable performance. Contrary to [8], the adaptive structure is not used to make the system robust against changes in Z_e but to keep good position and force tracking despite a high friction level, for a given value of Z_e. Our adaptive scheme is based on position and force measurements and no online estimation of Z_e is used. This paper is organized as follows. In section II, the theoretical developments are presented and the adaptive control structure is introduced. In section III, the experimental setup is described and used to validate the method experimentally. Finally, section IV provides the reader with some concluding remarks.

II. THE ADAPTIVE APPROACH

In this section, an adaptive 4C structure aimed at improving performance for high friction systems is presented. First, the adaptive approach is motivated based on practical considerations. Next, a more detailed representation of the 4C structure is proposed. This model makes explicit some conversion ratios, which are hidden in Z_h and Z_e in the model of figure 1. These coefficients, aimed at reducing the external forces (F_h and F_e) to the actuator axes, appear to be significant when studying the influence of friction on performance. Indeed, it is shown that some of these ratios are time-varying. So, in order to cope with this variation, an adaptive structure is defined. Finally, a preliminary study of stability is made for the obtained adaptive structure.

A. Motivation

In order to motivate the use of an adaptive 4C structure, let us consider the following reasoning for a one dof device without loss of generality. As it has been said in the introduction, Z_m is the Laplace transform of the force applied to the master (F_m) over the Laplace transform of its position (X_m). When considering figure 1, it appears that F_m is the sum of the actuator force (computed by the controller) and the force exerted by the user on the master (F_h). However, in a teleoperation system, the actuator and the loadcell measuring F_h are generally non-collocated. In figure 1, it is assumed that F_h is reduced to the actuator axis. In practice, a conversion ratio must be estimated to this end. It will be shown below that for high friction devices, this conversion ratio is time-varying and therefore an adaptive control structure is needed. The same reasoning applies for the slave with F_s, F_e and Z_s instead of F_m, F_h and Z_m respectively.

B. Extended representation of the 4C architecture

In order to address the practical aspects introduced in section II-A, which are not included in the model of figure 1, let us consider the model depicted in figure 2.

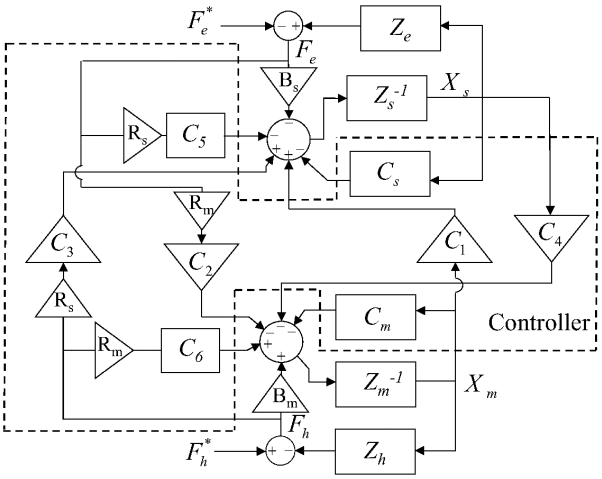

Fig. 2. Extended 4C control architecture

In order to simplify the drawing, $F_{s,actuator}$ and $F_{m,actuator}$ do not appear explicitly anymore. In this model the different conversion ratios denoted by B_m, B_s, R_m and R_s are represented. At this point, it is important to stress on the fact that B_m and B_s convert a physical external force into a physical torque[1] and are therefore not known a priori, while R_m and R_s are introduced in the controller to scale the electrical signal provided by the loadcell and are known exactly.

[1]Rotary actuators are assumed without loss of generality.

Let us first consider the system without local force loops, i.e. $C_5 = C_6 = 0$. It can be demonstrated that the ideal expressions of the communication channels are now given by (8).

$$\begin{array}{ll} C_1 = C_s + Z_s & C_2 = \frac{B_m}{R_m} \\ C_4 = -(C_m + Z_m) & C_3 = \frac{B_s}{R_s} \end{array} \tag{8}$$

A typical form for $Z_{\{m,s\}}$ is $M_{\{m,s\}}s^2 + N_{\{m,s\}}s$. Hence, if low frequency motions are assumed, Z_s and Z_m can be neglected in (8). The resulting control laws are given by expressions (9) and (10) where the estimated values $\hat{B}_s$ and $\hat{B}_m$ have been substituted for B_s and B_m respectively.

$$F_{m,actuator} = -\hat{B}_m F_e + C_m(X_s - X_m) \tag{9}$$

$$F_{s,actuator} = \hat{B}_s F_h + C_s(X_m - X_s) \tag{10}$$

Again, transparency can be obtained only if $\hat{B}_m = B_m$ and $\hat{B}_s = B_s$, which is not possible in practice due to model uncertainties.

C. Identification of the time-varying parameters

In this paragraph, experimental considerations will allow us to determine which parameters are time-varying in the representation of figure 2, when this linear model is used to approximately describe the behaviour of a high friction teleoperation system. As one can see, the control laws (9) and (10) can be decomposed into a position error term, and a force feed-forward term. R_s and R_m are canceled by the choice of communication channels which is not the case when considering local force loops as will be seen below. For a high friction teleoperation system, B_s and B_m are time-dependent. Indeed, consider two experiments carried out with the master arm alone and a rigid plate in order to evaluate B_m. It is assumed that a loadcell is available to measure the external force (F_h) and that the torque provided by the actuator ($F_{m,actuator}$) is known. In the first experiment, $C_{1,2,3,5,6,s} = 0$, $C_4 = -C_m \neq 0$ and $X_s = 0$, so the set point for X_m is zero. A disturbance on the master position is introduced by pressing a rigid plate at the robot tip (this experiment is depicted in figure 3).

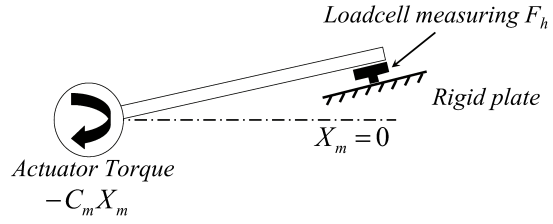

Fig. 3. Estimation of B_m (first experiment) in the case of a one dof rotary master arm

In the second experiment, all the channels are set to zero and the same plate is used. Initially, $F_{m,actuator} = 0$. It is then increased to a given value and the master comes into contact with the plate. For each experiment, an estimated value of B_m can be calculated at equilibrium by using the ratio $\frac{|F_{m,actuator}|}{F_h}$. It has been observed experimentally that this ratio is independent of the value of F_h. If the system was perfectly backdrivable, the ratios obtained from both experiments should be the same. When friction is present however, these two experiments give different values. Indeed, during the first experiment, friction is overcome by moving the plate while in the second experiment, friction is overcome by the actuator. For a given value of F_h, $|F_{m,actuator}|$ will be higher in the second case and so is B_m. The two experiments proposed above define two bounds, denoted by $B_{m,inf}$ and $B_{m,sup}$, between which the value of B_m varies during manipulation. The same reasoning applies to B_s for which two other bounds can be defined: $B_{s,inf}$ and $B_{s,sup}$. This justifies the introduction of an adaptive control structure where $\hat{B}_m$ and $\hat{B}_s$ are adapted in (9) and (10).

D. Generalization when $C_5 \neq 0$ and $C_6 \neq 0$

If local force loops are considered, i.e. $C_5 \neq 0$ and $C_6 \neq 0$, the ideal expressions for the four communication channels are given by (11).

$$\begin{array}{ll} C_1 = C_s + Z_s & C_2 = C_6 + \frac{B_m}{R_m} \\ C_4 = -(C_m + Z_m) & C_3 = C_5 + \frac{B_s}{R_s} \end{array} \tag{11}$$

Again, considering low frequency motions, the control laws are given by the following expressions where B_m and B_s have been replaced by their estimated values:

$$\begin{array}{c} F_{m,actuator} = C_6 R_m(F_h - F_e) - \hat{B}_m F_e \\ + C_m(X_s - X_m) \end{array} \tag{12}$$

$$\begin{array}{c} F_{s,actuator} = C_5 R_s(F_h - F_e) + \hat{B}_s F_h \\ + C_s(X_m - X_s) \end{array} \tag{13}$$

Contrary to the previous case, R_m and R_s now appear in the control laws and so, their value will influence stability. On the other hand, referring to figure 2, R_s and R_m are parts of the controller and there is no uncertainty on their value. In this work, R_m and R_s are chosen equal to $B_{m,sup}$ and $B_{s,sup}$ respectively, to express the forces at the input of the controller in actuator torque units.

E. Adaptation laws

The adaptation laws must now be chosen. The philosophy that will be used consists in adapting the control law of the slave in order to make the slave accurately track the motion of the master while the control law of the master will be adapted in order to make the user accurately feel the interaction force between the slave and its environment. For example, if the slave is behind the master during contact, it means that $\hat{B}_s$ is too low and should be increased in order to increase the torque provided by the actuator of the slave (see expressions (10) and (13)). $\hat{B}_m$ will be adapted in a similar way but based on the force error. This is formulated more formally below when local force loops are present. Define

$C_{2,sup} = C_6 + \frac{B_{m,sup}}{R_m}$ ($C_{2,inf} = C_6 + \frac{B_{m,inf}}{R_m}$), let the saturation function $sat_i(x)$ $(i = 2, 3)$ be defined as follows:

$$sat_i(x) = \begin{cases} C_{i,inf} & if \quad x \leq C_{i,inf} \\ x & if \quad C_{i,inf} < x < C_{i,sup} \\ C_{i,sup} & if \quad x \geq C_{i,sup} \end{cases}$$

and the sign function $sign(x, y)$ be defined as follows:

$$sign(x,y) = \begin{cases} -1 \; if & x, y < 0 \\ +1 \; if & x, y > 0 \\ 0 \; else & \end{cases}$$

Then, $C_2 = C_6 + \frac{B_m}{R_m}$ in (11) leads to the following adaptation law:

$$C_2 = C_6 + \frac{\hat{B}_m}{R_m} \tag{14}$$

$$= sat_2(C_6 + \frac{\hat{B}_m^0}{R_m} - K_2(F_h - F_e)sign(F_e, F_h)) \tag{15}$$

$$= sat_2(C_2^0 - K_2(F_h - F_e)sign(F_e, F_h)) \tag{16}$$

and similarly, if $C_{3,sup} = C_5 + \frac{B_{s,sup}}{R_s}$ ($C_{3,inf} = C_5 + \frac{B_{s,inf}}{R_s}$), $C_3 = C_5 + \frac{Bs}{R_s}$ in (11) yields the following adaptation law:

$$C_3 = C_5 + \frac{\hat{B}_s}{R_s} \tag{17}$$

$$= sat_3(C_5 + \frac{\hat{B}_s^0}{R_s} - K_3(X_s - X_m)sign(F_e, F_h)) \tag{18}$$

$$= sat_3(C_3^0 - K_3(X_s - X_m)sign(F_e, F_h)) \tag{19}$$

where K_2 and K_3 are parameters to be tuned and C_2^0, C_3^0, $\hat{B}_m^0$ and $\hat{B}_s^0$ are the nominal values of C_2, C_3, $\hat{B}_m$ and $\hat{B}_s$ respectively. As the adaptation is performed using the instantaneous value of the position and force errors, the adaptation rate is equal to the sampling rate of the process.

F. Preliminary stability study

A detailed stability study of this adaptive control scheme is necessary. Here, a preliminary stability study will be conducted by checking necessary but not sufficient stability conditions. In the defined structure, C_m, C_s, C_1, C_4, R_m, R_s, C_5, and C_6 are fixed but $C_2(\hat{B}_m)$, $C_3(\hat{B}_s)$, B_s and B_m are time-varying. If the different possible values of $C_2(\hat{B}_m)$, $C_3(\hat{B}_s)$, B_s and B_m are considered, a set of a time-invariant systems can be defined. Here a numerical stability check has been conducted on each element of the discretized set of time-invariant systems. The evaluation of stability for time-invariant teleoperation systems can be done using the SISO modeling proposed in [5] and also used in [2]. It consists in reducing the whole teleoperation system to a unique SISO transfer function placed in closed loop. The SISO transfer function is given by expression (20) and denoted by $P(s)$.

$$P(s) = \frac{h_{11} + (h_{12}h_{21} - h_{11}h_{22})Z_e}{(1 - h_{22}Z_e)Z_h} \tag{20}$$

In this expression, the hybrid parameters (h_{ij}) defined by expression (2), must be calculated using the model of figure 2. This formalism allows a straightforward estimation of stability as we only have to check if the closed-loop poles (i.e. the poles of $\frac{P(s)}{1+P(s)}$) remain in the left-half plane.

III. EXPERIMENTAL RESULTS

In this section, experimental results are presented to validate the concepts developed above.

A. Experimental setup

In order to implement the control structure developed in the previous section, a one dof teleoperation setup is used (see figure 4). It is made of two arms (length of $0.145\ mm$) moving like windscreen wipers. Each arm is actuated by a DC motor connected by a high friction gearbox (ratio of 20:1 with an average efficiency of 50%) and is equipped with a digital encoder ($USdigital^{TM}\ E2$) and a loadcell ($Honeywell^{TM}\ FSG$). The motor controllers are $Maxon^{TM}\ ADS\ 50/5$ controllers and the force and position measurements are sampled at a frequency of $1\ kHz$.

The identification of the impedances of the setup was

Fig. 4. Diagram of one arm of the teleoperation setup

performed using a frequency domain approach and a multisine excitation signal covering a frequency range from continuous to $15\ Hz$. Only the odd harmonics were excited and a random phase multisine was used in order to reduce the impact of the non-linearities of the system (see [9] for more details). The identified models are: $Z_m(s) = 0.17s^2 + 4.41s\ \ mNm/rad$, $Z_s(s) = 0.14s^2 + 2.94s\ \ mNm/rad$ and $Z_h(s) = \frac{11.5(0.0146s+1)}{0.0039s+1}\ N/rad$.

In the case of the human operator (Z_h), the matching between the experimental data and the results predicted by the model was satisfying only in the neighborhood of an operating point. This is due to the non-linear aspect of the human dynamics, depending on the grasping force and the position of the limbs for a given operator. During the experiments, the environment is constituted by two foam cylinders (stiffness of $800\ N/m$ and $2200\ N/m$ respectively).

B. Design of the controller

In our application, we will use proportional controllers with the control laws defined by (12) and (13) providing transparency only at low frequencies. The two experiments mentioned in paragraph II-C were performed with the slave and the master devices. The following bounds were identified:

$$4.23 \leq \hat{B}_s\ (mNm/N) \leq 11.54 \tag{21}$$

$$3.62 \leq \hat{B}_m \ (mNm/N) \leq 13.04 \tag{22}$$

The difference between the values for the master and the slave are due to slightly different friction levels and construction tolerance. If R_s is chosen equal to $11.54\ mNm/N$ and R_m to $13.04\ mNm/N$, then $0.278 \leq \frac{\hat{B}_m}{R_m} \leq 1$ and $0.366 \leq \frac{\hat{B}_s}{R_s} \leq 1$. To design the controllers, we need to define a nominal operating point. Based on our experience of the setup, $\frac{\hat{B}_s^0}{R_s}$ is chosen equal to 0.9 and $\frac{\hat{B}_m^0}{R_m}$ is chosen equal to 0.4. The controller parameters were manually tuned to provide maximum performance while keeping the system stable for the two possible values of environment stiffness: $C_5 = C_6 = -0.2$, $C_m = -C_4 = 395\ mNm/rad$ and $C_s = C_1 = 772\ mNm/rad$. C_5 and C_6 were chosen in the interval [-1,0], according to [6]. From these values, intervals for C_2 and C_3 are defined: $0.078 \leq C_2 \leq 0.8$ and $0.166 \leq C_3 \leq 0.8$. With our choice of nominal working point, we get $C_2^0 = 0.2$ and $C_3^0 = 0.7$. The values of K_2 and K_3 are given in the next section.

C. Implementation of the adaptive scheme.

Four experiments were performed by the first author. The adaptive controller was used for the first two experiments while no adaptation was performed during the last two, i.e. $K_2 = K_3 = 0$. The experimental parameters (parameters K_2 and K_3, which were manually tuned and environment stiffness), are presented in table I.

	Environment stiffness	K_2	K_3
Experiment 1	$800\ N/m$	$3.7\ N^{-1}$	$200\ rad^{-1}$
Experiment 2	$2200\ N/m$	$3.7\ N^{-1}$	$240\ rad^{-1}$
Experiment 3	$800\ N/m$	$0\ N^{-1}$	$0\ rad^{-1}$
Experiment 4	$2200\ N/m$	$0\ N^{-1}$	$0\ rad^{-1}$

TABLE I

PARAMETERS OF THE EXPERIMENTS

The experimental results are depicted in figures[2] 5 to 7 and the RMS of the position and force errors during contact are presented in table II. Although the force error during transients using the adaptive scheme seems to be quite important, especially for the higher stiffness (figure 6), both force and position trackings are improved, compared to the case were no adaptive structure is used.

	Exp. 1	Exp. 2	Exp. 3	Exp. 4
RMS position error	$0.10\ deg$	$0.11\ deg$	$0.55\ deg$	$1.21\ deg$
RMS force error	$0.22\ N$	$0.36\ N$	$0.58\ N$	$0.52\ N$

TABLE II

RMS OF THE POSITION AND FORCE ERRORS

[2]The plots of experiment 4 are not presented due to a lack of space. They are similar to these of experiment 3.

Notice however that, with the adaptive scheme, small vibrations were felt by the user during the experiments. Despite these vibrations and the poor force tracking during transients experienced with the adaptive structure, it appears clearly that an adaptation of $\hat{B}_m$ and $\hat{B}_s$ helps to keep suitable performance.

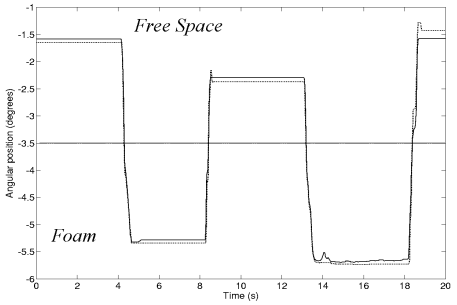

(a) Position of the master (continuous line) and the slave (dotted line)

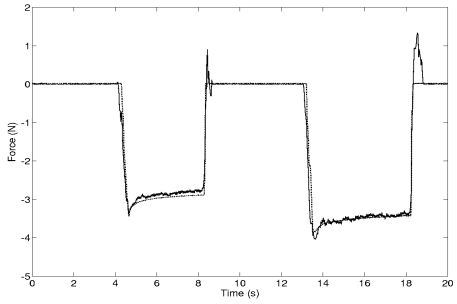

(b) Force of the master (continuous line) and the slave (dotted line)

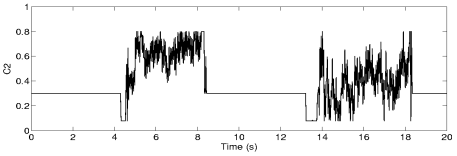

(c) Evolution of C_2

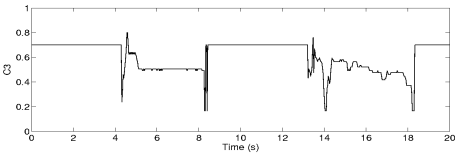

(d) Evolution of C_3

Fig. 5. First experiment: the environment is a foam cylinder placed at an angular position of $-3.5°$ and its stiffness is equal to $800\ N/m$.

IV. CONCLUSIONS AND FUTURE WORK

In this work, a new adaptive 4C structure aimed at improving performance in high friction devices is presented. First, based on a modified representation of the 4C structure including conversion ratios (B_m, B_s, R_m and R_s), it is shown that two coefficients of the system (B_m and B_s) are time-varying. Next, two experiments are proposed to identify the boundaries of the variation range of these parameters. A preliminary stability study of the resulting adaptive scheme is made and finally, the experimental results allowed us to

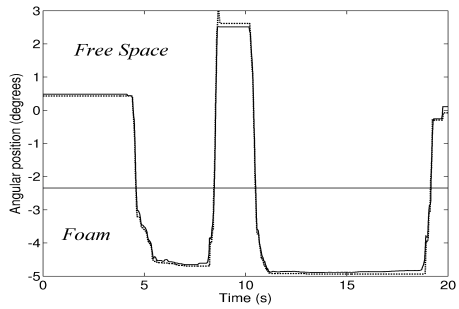

(a) Position of the master (continuous line) and the slave (dotted line)

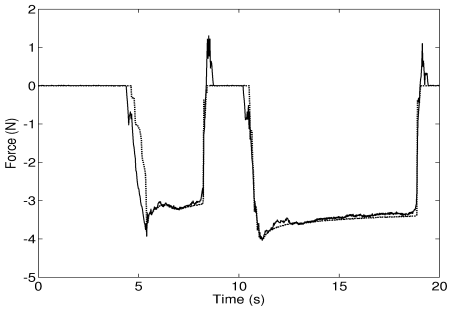

(b) Force of the master (continuous line) and the slave (dotted line)

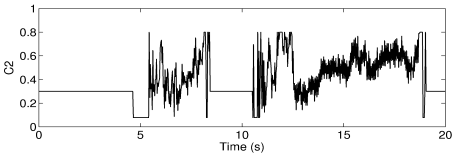

(c) Evolution of C_2

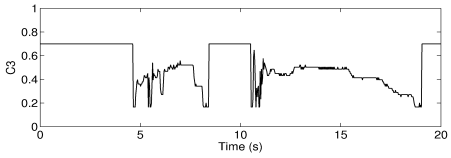

(d) Evolution of C_3

Fig. 6. Second experiment: the environment is a foam cylinder placed at an angular position of -2.34° and its stiffness is equal to 2200 N/m.

validate the proposed control approach.

Future work will include a stability study for the closed-loop time-varying system obtained with the adaptive control law. Moreover, although the experiments confirmed the need for an adaptive scheme, it should be useful to suppress the vibration phenomenon to allow comfortable and accurate haptic feedback and to improve force tracking during transients. To achieve this goal, the effect of higher control loop rates should be investigated and possibly alternative adaptation laws should be developed. Finally, the impact of variations of the parameters of Z_h on stability and performance should be investigated.

V. ACKNOWLEDGMENTS

The work of Thomas Delwiche is supported by a FRIA (Fonds pour la Formation à la Recherche dans l'Industrie et l'Agriculture) grant.

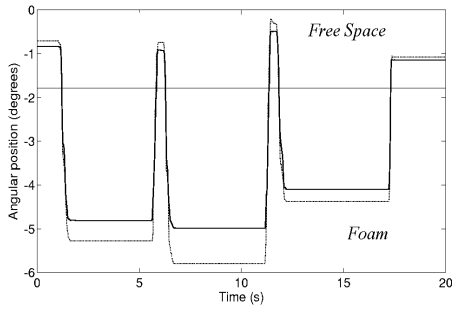

(a) Position of the master (continuous line) and the slave (dotted line)

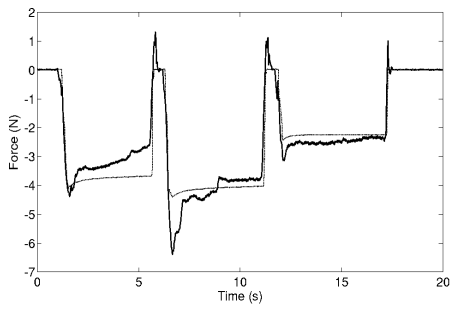

(b) Force of the master (continuous line) and the slave (dotted line)

Fig. 7. Third experiment : the environment is a foam cylinder placed at an angular position of -1.8° and its stiffness is equal to 800 N/m. No adaptation of the parameters is used.

REFERENCES

[1] I. Aliaga, A. Rubio, and E. Sánchez. Experimental quantitative comparison of different control architectures for master-slave teleoperation. *IEEE transactions on control systems technology*, 12(1):2–11, 2004.

[2] M.C. Çavusoglu, A. Sherman, and F. Tendick. Design of bilateral teleoperation controllers for haptic exploration and telemanipulation of soft environments. *IEEE transactions on robotics and automation*, 2002.

[3] P. Coiffet and A. Kheddar. *Téléopération et télérobotique*. Hermès science publications, 2002.

[4] B. Hannaford. A design framework for teleoperation with kinesthetic feedback. *IEEE transaction on robotics and automation*, 5(4):426–434, 1989.

[5] B. Hannaford. Stability and performance tradeoffs in bi-lateral telemanipulation. *Proceedings of the IEEE International Conference on Robotics and Automation, Scottsdale, AZ*, 3:1764–1767, May 1989.

[6] K. Hashtrudi-Zaad and S.E. Salcudean. On the use of local force feedback for transparent teleoperation. *Proceedings of the IEEE international conference on robotics and automation*, pages 1863–1869, 1999.

[7] D.A. Lawrence. Stability and transparency in bilateral teleoperation. *IEEE transactions on robotics and automation*, 9(5):624–637, 1993.

[8] L.J. Love and W.J. Book. Force reflecting teleoperation with adaptive impedance control. *IEEE transactions on systems, man and cybernetics*, 34(1):159–165, 2004.

[9] R. Pintelon and J. Schoukens. *System identification, a frequency domain approach*. IEEE Press, 2001.

[10] Y. Yokokojhi and T. Yoshikawa. Bilateral control of master-slave manipulators for ideal kinesthetic coupling - formulation and experiment. *IEEE transactions on robotics and automation*, 10(5):605–619, 1994.

[11] W. Zhu, S.E. Salcudean, and M. Zhu. Experiments with transparent teleoperation under position and rate control. *IEEE International Conference on Robotics and Automation*, pages 1870–1875, 1999.